Int J Earth Sci (Geol Rundsch) (2017) 106:255–268
DOI 10.1007/s00531-016-1315-2

ORIGINAL PAPER

Constraining the alteration history of a Late Cretaceous Patagonian volcaniclastic bentonite–ash–mudstone sequence using K–Ar and $^{40}Ar/^{39}Ar$ isotopes

L. N. Warr[1] · H. Hofmann[2] · B. A. van der Pluijm[3]

Received: 15 April 2015 / Accepted: 26 February 2016 / Published online: 21 March 2016

Abstract Smectite is typically considered unsuitable for radiometric dating, as argon (^{40}Ar) produced from decay of exchangeable potassium (^{40}K) located in the interlayer sites can be lost during fluid–rock interaction and/or during wet sample preparation in the laboratory. However, age analysis of Late Cretaceous Argentinian bentonites and associated volcaniclastic rocks from Lago Pellegrini, Northern Patagonia, indicates that, in the case of these very low-permeability rocks, the radioactive ^{40}Ar was retained and thus can provide information on smectite age and the timing of rock alteration. This study presents isotopic results that indicate the ash-to-bentonite conversion and alteration of the overlying tuffaceous mudstones in Northern Patagonia was complete ~13–17 my after middle Campanian sedimentation when the system isotopically closed. The general absence of illite in these smectite-rich lithologies reflects the low activity of K and the low temperature (<60 °C) of the formation waters that altered the parent ash.

Keywords Smectite age dating · K–Ar and $^{40}Ar/^{39}Ar$ isotopes · Cretaceous ash · Bentonite · Tuffaceous mudstone · Detrital mica · Neuquén Basin · Argentina

Introduction

The smectite group of clay minerals is ubiquitous to the Earth's surface and upper crust environment and results from water–rock interaction in sedimentary, igneous and metamorphic rocks at low temperatures (<60 °C) that has occurred through most of the Earth's history (Christidis and Huff 2009; Hazen et al. 2013). The weakly charged interlayers of smectite contain exchangeable cations, typically Na, K, Ca and Mg, which are often present in only small quantities (<2 % weight oxides). The small concentrations of exchangeable K in smectite layers typically occur in the lower-layer charged smectites (Bergaya et al. 2006) and in decreasing amounts within the variably charged smectitic layers of illite–smectite minerals (Środoń et al. 1986).

Despite containing exchangeable K, smectites are generally not considered to be suitable for K–Ar or $^{40}Ar/^{39}Ar$ radiometric dating due to poor ^{40}Ar retention (McDougall and Harrison 1999) and the difficulties in accurately measuring the small quantities of ^{40}K and radiogenic ^{40}Ar involved. The radiogenic ^{40}Ar produced is more weakly held in hydrated low-charge interlayer sites and can be lost from the fine-grained clay mineral phases during subsequent fluid–rock interaction and recrystallization events. Although less studied, radiogenic ^{40}Ar in smectite may also be lost during sample preparation, as do various K-bearing sheet silicate phases treated by acid, strong dispersive or grinding methods (Aronson and Douthitt 1986; Nauman et al. 2012). Conversely, some experimental heating studies suggest smectite can have a similar retention potential

Electronic supplementary material The online version of this article (doi:10.1007/s00531-016-1315-2) contains supplementary material, which is available to authorized users.

✉ L. N. Warr
warr@uni-greifswald.de

H. Hofmann
post@heikohofmann.de

[1] Institute of Geography and Geology, Ernst-Moritz-Arndt-University Greifswald, Friedrich-Ludwig-Jahn-Str. 17a, 17487 Greifswald, Germany

[2] Binzener Strasse 11k, 79539 Lörrach, Germany

[3] Department of Earth and Environmental Sciences, University of Michigan, 1100 N. University Ave, Ann Arbor, MI 48109, USA

to illite and glauconite, with radiogenic ^{40}Ar remaining to about 250 °C (Odin and Bonhomme 1982; Hassanipak and Wampler 1996). That smectite can retain its ^{40}Ar was supported by a K–Ar and Rb–Sr study of detrital smectites from Atlantic sediments that yielded systematically older ages than the age of their sedimentation (Clauer et al. 1984). As the amount of exchangeable and non-exchangeable K was not determined in the study, some uncertainly remains as to whether such smectites were truly free of illite layers.

In contrast to smectite, the fixed K content of illite has been widely used to date low-temperature diagenetic, hydrothermal and faulting events in the geological record by illite age analysis using both K–Ar and ^{40}Ar/^{39}Ar isotopes (e.g., Hunziker et al. 1986; Pevear 1992; van der Pluijm et al. 2001; Bechtel et al. 1999; Clauer et al. 2012; Clauer 2013). A range of grain sizes is extracted from the rocks that contain various mixtures of authigenic illite characterized by one-layer monoclinic polytypes (1 M or the disordered $1M_d$ variety) and detrital illite normally of the two-layer monoclinic ($2M_1$) polytype (Smith and Yoder 1956). On the basis of linear extrapolation to end-member fractions, the age of diagenetic and detrital phases can be obtained from mixed illite age verses % detrital ($2M_1$) illite plots, for example, with the aid of improved quantification methods of polytypes (Grathoff and Moore 1996). The illite age analysis approach has been advanced to reduce the nonlinearity in the graphs by plotting the isotopic ages as the function: $\exp(\lambda t)$-1 (where t is time and λ the decay constant; van der Pluijm et al. 2001) or by introducing other procedures to account for the varying concentrations of K in authigenic and detrital phases (Szczerba and Srodon 2009). The validity of the $\exp(\lambda t)$-1 plotting approach has been demonstrated using artificial mixtures of illite and muscovites of varying K concentrations and of known ages (Haines and van der Pluijm 2008).

In order to investigate whether the alteration of very low-permeability ($<10^{-11}$ m^2/s) smectite-dominated rocks can be dated, we selected a suite of closely associated montmorillonite-rich lithologies from a Late Cretaceous volcaniclastic sequence that is well exposed in freshly cut clay pits along the southern shoreline of the Lago Pellegrini Lake, close to Neuquén, Northern Patagonia (Fig. 1a). This location was selected due to the high purity of the bentonite samples, containing 85–98 % Na-montmorillonite, high cation exchange capacities of 45–68 (meq/100 g) and the occurrence of exchangeable K in the concentration range of 0.08–0.92 (meq/100 g) (Lombardi et al. 2003; Iborra et al. 2006). The rocks are particularly interesting for a test of smectite dating because initial X-ray diffraction analyses of these samples did not detect illitic mixed layers (Lombardi et al. 2003; Iborra et al. 2006; Hofmann 2003).

Based on the K–Ar and ^{40}Ar/^{39}Ar age analysis of the whole-rock powders, we present results that indicate the authigenic smectite in this Cretaceous volcaniclastic sequence can be dated, and provide some first age constraints for the time period required to convert an ash into a Na-bentonite deposit. It also produces relevant information on how long a compacted bentonite may remain isotopically closed at shallow crustal depth, a topic of current relevance to the underground disposal of radioactive waste.

Geological setting

The study area is located in the Neuquén sedimentary basin situated to the east of the Andean mountains (Fig. 1a). Three stages of basin development are recognized along the eastern Gondwana margin (Howell et al. 2005): (1) Late Triassic to Early Jurassic continental crustal extension, (2) Early Jurassic to Early Cretaceous thermal subsidence in a backarc setting related to the development of a steep subduction zone and (3) Late Cretaceous

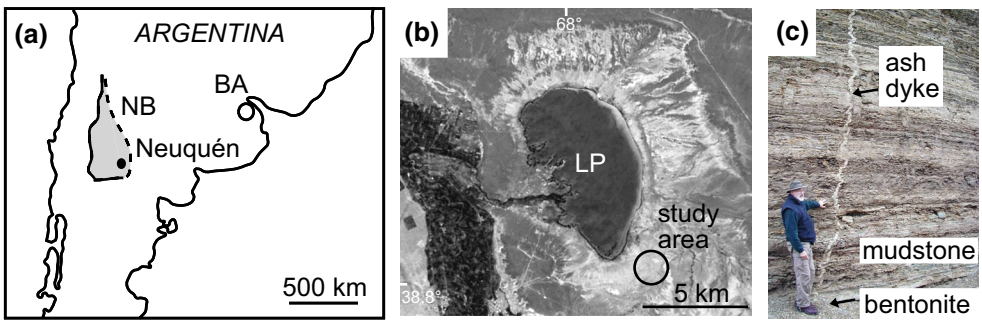

Fig. 1 **a** Map of Northern Patagonia (Argentina) showing the study location, close to the town of Neuquén. *NB* Neuquén Basin, *BA* Buenos Aires. **b** Satellite image of the Lago Pellegrini showing the study area along the southeastern scarp of the lake, ~15 km north of Neuquén (*source* http://www.nasa.gov/home/index.html). **c** Field photograph of the bentonite, ash dyke and tuffaceous mudstone lithologies, which were sampled within 3 m range

to Cenozoic backarc compression and foreland flexure caused by a shallowing of the subduction. The ~7-km-thick basin fill contains economically important clay deposits including a series of relatively pure bentonite horizons of Upper Cretaceous to Tertiary age derived from volcanic ashes originating from the Andean chain (Lombardi et al. 2003).

The bentonite pit studied lies within a volcaniclastic sequence located along the southeastern shoreline of Lake Pellegrini, ~25 km north of the town of Neuquén (Fig. 1b). The pit exposes the middle section of the Upper Cretaceous Allen Formation (Malargüe group), which represents a transitional littoral marine sedimentary sequence characterized by the deposition of a number of glass-bearing pyroclastic ash layers, most of which have been almost entirely altered to bentonite (Vallés et al. 1989; Vallés and Giusiano 2001; Impiccini 1995). Based on the paleontology of the formation, the 52- to 54-m-thick succession was deposited during Campanian to Lower Maastrichtian times (Vallés et al. 1989). The economically important clay layers are laterally persistent over many kilometers and range between 0.15 and 0.7 m thick.

The locality is also of special interest as one of the mined <1 m bentonite horizons occurs together with its parent ash, which is preserved as syn-compactional ash dykes that intruded upward from the bentonite layer (prior to its alteration) along subvertical fractures in the overlying mudstones (Fig. 1c). These ash dykes formed within an overpressured environment and were themselves compacted by a further ~30 % prior to lithification. All three lithologies were sampled within short distance of each other (<3 m) and are very fine-grained rocks in appearance. The bentonite clay rock is whitish to pale greenish in color, the mudstone is medium gray, and of probable volcaniclastic, tuffaceous, origin and the pyroclastic ash is light gray, with a slightly coarser texture. The ash dyke is significantly less altered than the bentonite and mudstone lithologies, probably because it was intruded vertically to the bedding anisotropy and was partly sealed by clay smears along the dyke walls. This part of the sequence belongs to the middle member of the Allen Formation (Malargüe Group) that was deposited during the Late Cretaceous, which, based on palynological findings, is considered to belong to the middle Campanian stage (cited as personal communication in Gasparini et al. 2001) with an absolute age placed between 80.3 and 76.2 Ma (Gradstein et al. 2004). Although SHRIMP U–Pb stratigraphic dating of zircons is available from tuffs higher up in the Malargüe Group of the Neuquén Andes (Aguirre-Urreta et al. 2011), such constraints do not exist from the studied volcaniclastic sequence.

Analytical methods

Sample treatment

The samples collected in the field were sealed in plastic bags and placed under laboratory conditions to avoid excessive drying. Each ~300–500 g sample was split into 2 parts (a and b) and then treated and analyzed separately to test for reproducibility. A proportion of each soft sample was gently crushed by hand in a pestle and mortar to produce a fine-grained powder and then returned to sealed containers. This gentle physical treatment is not considered to have modified the material in any significant way.

Major element composition and mineral assemblage

The major element composition of the powders was determined by X-ray fluorescence (XRF) using a Philips PW2404 X-ray spectrometer and 800 mg of dry powdered sample. The mass loss was measured after heating to 105 °C (20 h) and 1050 °C (1 h) to determine the loss on ignition (LOI). The remaining sample was melted with a flux ($LiBO_2 + Li_2B4O_7$) at about 1100 °C to prepare the tablet used for measurement. The data set was finally normalized to 100 % to remove the diluting effects of interlayer water in smectite that was not effectively removed at 105 °C (Table 1). The accuracy of measurements was controlled using available USGS standards (BHVO-2, AGV-2 and RGM-1).

The mineral assemblage of each sample portion was furthermore characterized by random powder X-ray diffraction (XRD) analysis and then by study of the <2-μm grain size fraction as textured slides. Both whole-rock powders and the <2-μm size fractions were prepared in the air-dried, ethylene glycol saturated and heat-treated state. The weight % of the <2-μm size fraction was determined by repeat separation by centrifuge until the suspension was clear. The <2-μm and >2-μm size fractions were then dried at 60 °C, and the dry weight % determined. Representative untreated bentonite, ash and mudstone lithologies were also selected for layer charge determinations using the alkylammonium method of Lagaly and Weiss (1971). A detailed description of the sample and alkylammonium chloride solution preparation procedure can be found in Mermut and Lagaly (2001). This method allows the layer charge distribution of expandable clay mineral phases to be determined and to test whether any illitic layers are recognizable in these samples. Freeze-dried samples (0.1 g) were homogenized twice in alkylammonium chloride solutions (4 mL) with carbon chain lengths from nC = 3 to nC = 18 (except nC = 17) and then washed at least eight times with 5 mL of pure ethanol. As an internal standard for calibration, 10 % of talc

Table 1 Mean oxide weight % compositions of the volcaniclastic sample set based on XRF analysis

Sample	Lithology	N	SiO_2	TiO_2	Al_2O_3	Fe_2O_3	MnO	MgO	CaO	Na_2O	K_2O	Sum %
arg 1	Bentonite	2	62.75	1.23	22.06	4.42	0.01	2.10	2.45	4.47	0.51	100.00
arg 5	Bentonite	2	65.33	0.17	21.88	5.23	0.02	3.26	0.18	3.66	0.27	100.00
arg 11	Bentonite	2	66.39	0.18	21.50	4.71	0.02	3.42	0.89	2.62	0.27	100.00
arg 2	Ash	2	76.79	0.67	13.15	2.12	0.01	1.05	1.08	3.50	1.62	100.00
arg 8	Ash	2	76.84	0.65	13.23	2.37	0.02	1.17	1.26	2.95	1.50	100.00
arg 10	Ash	2	68.38	0.66	16.72	3.52	0.04	1.53	4.14	3.57	1.44	100.00
arg 3	Mudstone	2	67.58	0.72	18.43	5.45	0.03	2.49	0.45	3.39	1.47	100.00
arg 6	Mudstone	2	65.89	0.66	18.16	6.19	0.18	2.57	1.50	3.50	1.35	100.00
arg 7	Mudstone	2	68.00	0.69	17.83	5.66	0.04	2.54	0.47	3.39	1.37	100.00
arg 9	Mudstone	2	70.13	0.76	17.03	4.68	0.03	2.10	0.90	2.84	1.53	100.00
Standards												
BHVO-2	Measured	4	49.51	2.73	13.47	12.34	0.17	7.32	11.54	2.39	0.52	100.00
BHVO-2	Standard values	–	49.9	2.73	13.50	12.30	0.167	7.23	11.40	2.22	0.52	99.97
	% Difference		−0.78	0.00	-0.22	+0.33	+1.80	+1.24	+1.23	+7.66	0.00	–
AGV-2	Measured	4	60.07	1.06	17.28	6.90	0.10	1.81	5.38	4.45	2.96	100.00
AGV-2	Standard values	–	59.30	1.05	16.91	6.69	0.10	1.79	5.20	4.19	2.88	98.11
	% Difference		+1.30	+0.95	+2.19	+3.14	0.00	+1.12	+3.46	+6.21	+2.78	–
RGM-1	Measured	4	73.53	0.26	13.84	1.83	0.04	0.30	1.27	4.52	4.42	100.00
RGM-1	Standard values	–	73.45	0.27	13.72	1.88	0.04	0.28	1.15	4.07	4.30	99.15
	% Difference		+0.11	+3.70	+0.87	−2.66	0.00	+7.14	+10.43	+11.06	+2.79	–

The % values were normalized to 100 % to remove the diluting effects of remaining interlayer water. *N* = number of analyses

(<2 mm fraction) was added. Oriented samples were prepared for XRD analysis by pipetting 1 mL of the dispersion onto glass slides and air-dried at 60 °C overnight before dehydrated under vacuum conditions over P_2O_5 in a dessicator for a further 24 h. For layer charge determination, oriented samples were measured using either a Siemens D500 or Bruker AXS D8 diffractometer. To reduce water uptake and swelling caused by humidity, the samples were measured individually, while other samples were stored under vacuum conditions. The *d* values of X-ray diffraction (001) smectite reflections that provide a measure of lattice layer thicknesses were plotted as a function of the number of carbon atoms in the alkyl chain. From these results the average charge density and layer charge distribution were calculated using the program XCharge (Hofmann et al. 2002), following the calculation procedure of Lagaly (1994).

K–Ar dating of whole-rock powders

Portions of the whole-rock powders not subjected to any treatment other than crushing were analyzed by the conventional K–Ar dating technique (Dalrymple and Lanphere 1969). The samples were crushed by hand, dried at room temperature and at no time brought into contact with water. Any loss of radiogenic Ar is considered unlikely to have occurred during this stage of sample preparation. The K–Ar method was selected to enable relatively large quantities of sample to be analyzed and thus to reduce the effects of sample heterogeneity. This method also avoids the potential of recoil when irradiating very fine-grained clay samples for $^{40}Ar/^{39}Ar$ (Clauer 2013). For measurements of Ar used for the K–Ar analysis, samples were pre-heated under high vacuum at 100 °C for at least 12 h to reduce the amount of atmospheric ^{36}Ar adsorbed on the mineral surfaces. The Ar extractions were made in a glass extraction line following a method similar to that used by Bonhomme et al. (1975). The method involves addition of a ^{38}Ar spike and control of the $^{40}Ar/^{36}Ar$ ratio (295.5) of the atmospheric Ar for both the blank of the extraction line and the mass spectrometer whereby the peak heights vary as a function of mass (mass discrimination). The analytical accuracy was also controlled by frequent measurement of the international GL-O standard (K concentration = 6.56 ± 0.06 wt% after Odin, 1982), which averaged 24.38 ± 0.12 × 10–6 cm^3/g STP (2σ) of radiogenic ^{40}Ar (^{40}Ar rad). All values were close to the theoretical levels, so no corrections were made to the analytical data.

As all the samples measured contained low concentrations of ^{40}Ar, particular attention was given to the precision and accuracy of the measurements. Repeat analyses of the same sample powders during the course of the study showed close to no variations in the results obtained, whereas repeat analyses of the (a) and (b) powder preparations made from different portions of the same samples

produced average variations of ~5 % (1σ). No noticeable decrease in the precision of measurement was recognizable with decreasing K content, probably because all samples contain low concentrations of this element ($K_2O \leq 1.18$ %). This degree of error is very similar to the ~4.4 % analytical accuracy determined by repeat measurement of the GLO standard. In most cases a sample weight of between 20 and 30 mg was sufficient to attain reproducible results within the range of errors mentioned. However, for the bentonite samples with $K_2O \leq 0.51$ %, the low concentrations of radiogenic ^{40}Ar gas were determined by taking the average of up to three batches of ~30 mg in order to improve measurement statistics.

K_2O measurements and determination of fixed and exchangeable K content

A significant source of error in the K–Ar method may be caused by the accuracy of measuring K_2O. Therefore, three different methods of K determination were compared: atomic absorption, inductively coupled plasma–mass spectrometry and XRF (supplementary data A). The most accurate data set (<2.8 % error), used in this study, was determined by XRF and control using USGS standards BHVO-2 ($K_2O = 0.52$ %), AGV-2 ($K_2O = 2.88$ %) and RGM-1 (4.07 %): Table 1. This method has the advantage of measuring larger sample amounts (800 mg) that help average out sample heterogeneities. Powders were measured also after removal of the exchangeable K. This was achieved by exchanging with 1 M ammonium acetate solution, followed by exchange with 1 N $CaCl_2$. Each exchange was performed 4 times before washing of the powders by dialysis. The amount of exchangeable K (K_2O exch.) was calculated from the difference between the non-exchanged (K_2O %) and the exchanged sample (K_2O fixed), whereas the amount of fixed K (K_2O fixed) is equivalent to the remaining concentration of the exchanged material (Table 2).

K_2O determination and 40Ar/39Ar dating of the pure mica fraction

A pure mica fraction was obtained from the least altered ash sample (arg 2) by wet sieving of the powdered material

Table 2 Mineralogical, compositional and radiogenic isotope results determined for ten whole-rock powders and one mica separate from the Late Cretaceous volcaniclastic rocks of the Lago Pellegrini

Sample	Lithology	Mineralogy	K_2O (%)	K_2O exch.	K_2O fixed	Mica[a] (%)	^{40}Ar (10^{-6} cc/g)	^{40}Ar (%)	Age (Ma)
arg 1	Bentonite	Mnt, Pl, Ms, Bt	0.51	0.07	0.45	5.56 ± 0.27	1.20	11.65	70.9 ± 3.2 (4.6 % error)
arg 5	Bentonite	Mnt, Pl, Ms, Bt	0.27	0.07	0.20	2.44 ± 0.44	0.68	4.20	76.7 ± 4.4 (5.7 % error)
arg 11	Bentonite	Mnt, Pl, Ms, Bt	0.27	0.04	0.23	2.18 ± 0.09	0.56	3.30	63.2 ± 3.0 (4.6 % error)
arg 2	ash	Qz, Pl, Hul/Cpt, Mnt, Ms, Bt	1.62	0.20	1.42	17.81 ± 0.44	6.05	48.75	112.5 ± 4.4 (3.9 % error)
arg 8	ash	Qz, Pl, Hul/Cpt, Mnt, Ms, Bt	1.50	0.16	1.34	16.69 ± 0.44	5.65	47.60	113.8 ± 4.4 (3.9 % error)
arg 10	ash	Qz, Pl, Hul/Cpt, Mnt, Ms, Bt	1.44	0.10	1.34	16.75 ± 0.88	4.08	38.85	94.3 ± 4.0 (4.2 % error)
arg 3	Mudstone	Mnt, Qz, Pl, Ms, Bt	1.48	0.07	1.41	17.63 ± 0.18	4.98	30.25	101.7 ± 4.0 (3.9 % error)
arg 6	Mudstone	Mnt, Qz, Pl, Ms, Bt	1.36	0.07	1.29	16.13 ± 0.18	3.90	25.35	86.6 ± 3.5 (4.0 % error)
arg 7	Mudstone	Mnt, Qz, Pl, Ms, Bt	1.38	0.04	1.33	16.63 ± 0.18	5.25	26.30	115.0 ± 4.3 (3.7 % error)
arg 9	Mudstone	Mnt, Qz, Pl, Ms, Bt	1.53	0.13	1.41	17.56 ± 0.62	5.65	35.88	111.2 ± 4.6 (4.1 % error)
arg 2	Separates	Ms. Bt	8.0	–	8.0	100.00 ± 0.00	–	–	260.6 ± 7.2[b] 2.8 % error

All values for powdered samples are the averages of two measurements per sample

Mnt montmorillonite, *Pl* plagioclase, *Ms* muscovite, *Bt* biotite, *Qz* quartz, *Hul/Cpt* heulandite/clinoptilolite. *exch.* exchangeable, *fixed* fixed (non-exchangeable)

[a] Error calculated based on 4.4 % accuracy for the method

[b] Based on total gas age of $^{40}Ar/^{39}Ar$ spectrum

and hand picking of micas from the 160- to 250-μm fraction using a needle. Approximately 60 mica grains were selected and used for $^{40}Ar/^{39}Ar$ analysis of samples wrapped in the (Al) foil following published procedures (LoBello et al. 1987). About 30 mica grains were also mounted for scanning electron microscopy (SEM) study, which was made using a Zeiss Auriga SEM–FIB instrument equipped with an extra large 80-mm^2 CCD detector for improved energy-dispersive X-ray spectroscopy analyses. The average K_2O % content was determined based on 118 analyses of selected areas of the mica grains that are free of contamination. The analyses were calibrated using machine standards and verified by measurement of selective mineral standards. The accuracy of this approach was between 4 and 5 % (1σ confidence level).

Transmission electron microscopy

The same sample of ash (arg 2) was also studied by transmission electron microscopy in order to examine the nature of the lattice layers using fringe imaging of an ion-milled sample. The analytical methods used are described in Solum et al. (2003) and using the LR white resin impregnation method of Kim et al. (1995) to maintain the expandable state of smectite under the vacuum of the microscope.

Results

Sample composition

The elemental composition of the bentonite, ash and mudstone samples determined by XRF (Table 1) shows considerable variations between lithologies that are related primarily to the degree of rock alteration and the abundance of smectite. The parent ash samples are notably high in SiO_2 (68.38–76.79 %) but relatively low in Al_2O_3 (13.15–16.72 %) and MgO (1.05–1.53 %). In contrast, the bentonites are notably lower in SiO_2 (62.75–66.39 %) and as expected are enriched in Al_2O_3 (21.50–22.06 %), Fe_2O_3 (4.42–5.23 %) and MgO (2.10–3.42 %). The compositions of the mudstone samples in general appear intermediate between that of the ash and bentonites lithologies. Less expected are the similar concentrations of Na_2O in all samples. The cause of the variation in CaO content is also not so evident, but may relate to trace amounts of gypsum detected in some samples. The concentration of K_2O is clearly lowest in the bentonite samples (0.27–0.51 %) and has a relatively consistent, but higher concentration in the ash and mudstone samples (1.25–1.62 %). The highest K_2O value of 1.62 % was recorded in ash sample arg 2, which also gives the lowest Al_2O_3 value of 13.15 %. This sample

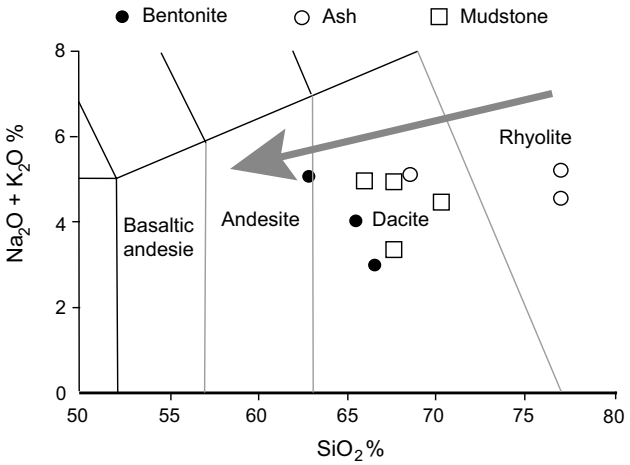

Fig. 2 Igneous classification of the Upper Cretaceous volcaniclastic rocks from the Lago Pellegrini, Argentina, based on the discrimination plot of LeBas et al. (1986). Only the relevant area of the la Bas plot is shown. *Arrow* shows the trend toward increasing rock alteration

is considered to represent the least altered ash and was studied in more detail by electron microscopy.

An attempt to determine the composition of the volcaniclastic rocks was made using major weight % oxides and the discrimination diagram of LeBas et al. (1986) for volcanic rocks. Plotting $Na_2O + K_2O$ (%) versus SiO_2 (%), the ash samples fall in the dacite–rhyolite field, the mudstone sample in the dacite field and the bentonite in the andesite–dacite field (Fig. 2).

As the decrease in SiO_2 corresponds to increasing amounts of Al_2O_3, Fe_2O_3 and MgO related to leaching and smectite growth during progressive alteration, the parent ash was probably more acidic in composition. However, as the ash contains detrital mica, it cannot be ruled out that a certain volume of the quartz in this lithology may also be of detrital origin. Additionally, some crystal fractionation may have also occurred during injection of the ash dyke, whereby the less dense minerals, such as quartz, may have been more mobilized and concentrated. As a result, the identification of the parent volcanic rock type based on the major elements is here not considered as being conclusive.

Sample mineralogy

Mineralogical study of 10 smectite-rich samples (3 bentonite, 3 ash and 4 mudstones: Table 2) by XRD and SEM shows variable mixtures of Na-montmorillonite smectite, plagioclase feldspar, quartz and minor amounts of mica. In general, the simplest mineral assemblage is that of the bentonite, which contains abundant (>90 %) Na-montmorillonite, with minor plagioclase and mica. In contrast, the ash is dominated by quartz, plagioclase and mica, with

significantly lesser amounts of Na-montmorillonite. A zeolite mineral of the heulandites/clinoptilolite series occurs as an additional authigenic phase in this lithology (Fig. 3). The mudstone lithology has a similar mineralogy to the bentonite except for the abundance of quartz and higher proportion of mica. No other clay mineral, other than Na-montmorillonite was detected in any of the samples, as evident by ethylene glycol-treated samples (Fig. 3) where the 001 XRD reflection swells to 1.7 nm, typical of a pure smectite phase (Moore and Reynolds 1997).

The pure nature of these smectite phases and absence of interlayer illite was confirmed by layer charge distributions measurements and the formation of monolayer alkyl ammonium structures. The bentonite sample (arg 11) is characterized by a smectite phase with a low change ranging between 0.19 and 0.37 eq/$(Si,Al)_4O_{10}$ and a mean charge of 0.26 eq/$(Si,Al)_4O_{10}$ (Fig. 4a). Both the ash (arg 8) and mudstone samples (arg 9) are characterized by slightly higher smectite layer charges, which range between 0.22 and 0.50 eq/$(Si,Al)_4O_{10}$ and both averaged 0.30 eq/$(Si,Al)_4O_{10}$ (Fig. 4b, c). Only in the ash sample was a high-layer charged phase detected (Hofmann 2003), with the development of palisade alkyl ammonium structures. This distinct phase is attributed to the higher concentrations of muscovite and biotite recognized in this sample (Table 2).

Based on SEM compositional analyses, only two K-bearing mineral phases were recognized in variable amounts. They are characterized by (1) high concentrations of K in micas of low abundance (Fig. 5a) and (2) low concentrations of K in abundant Na-montmorillonite smectite (Fig. 5b). The most abundant type of mica is that of muscovite, but the mica fraction also includes some biotite. As these minerals are generally irregular in shape and show signs of crystal damage, they are considered

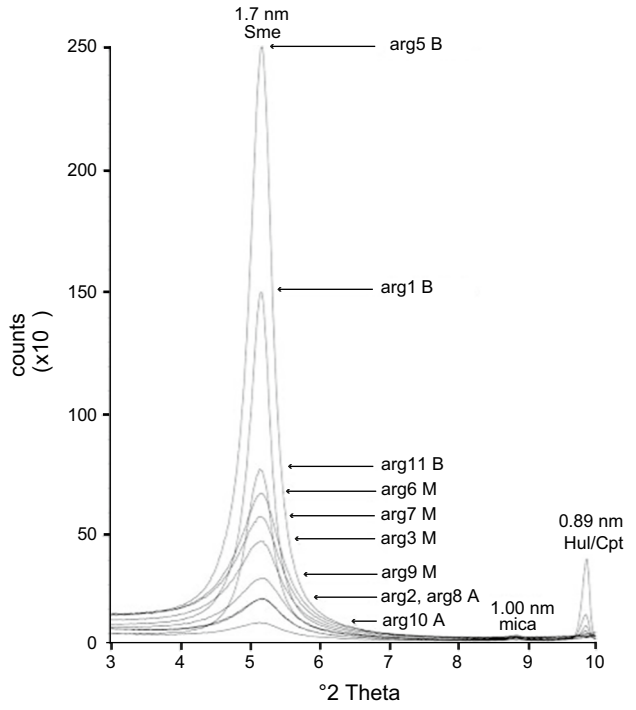

Fig. 3 X-ray diffraction patterns of the low-angle 2θ range (3–10 °C) of ethylene glycol saturated, textured preparations of the volcaniclastic samples, showing the position of the *001* smectite (Sme) reflections at ~1.7 nm, weak mica reflections at 1.00 nm and the occasional occurrence of a 0.89-nm reflection attributed to a zeolite of the heulandite/clinoptilolite (Hul/Cpt) series

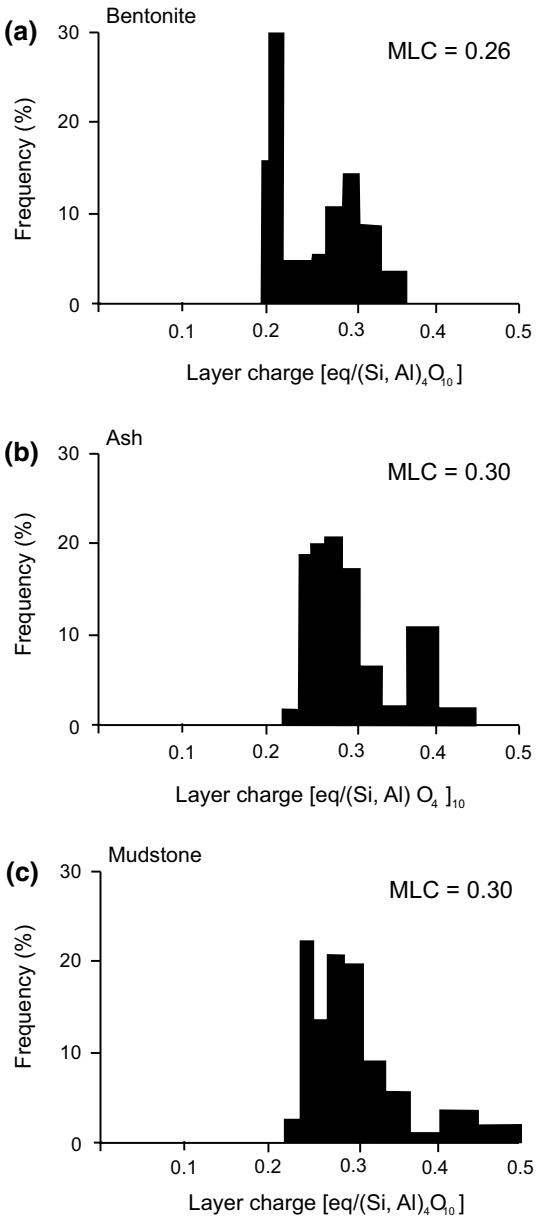

Fig. 4 Layer charge distribution of smectitic clay mineral phases of representative **a** bentonite, **b** ash and **c** mudstone samples. *MLC* mean layer charge

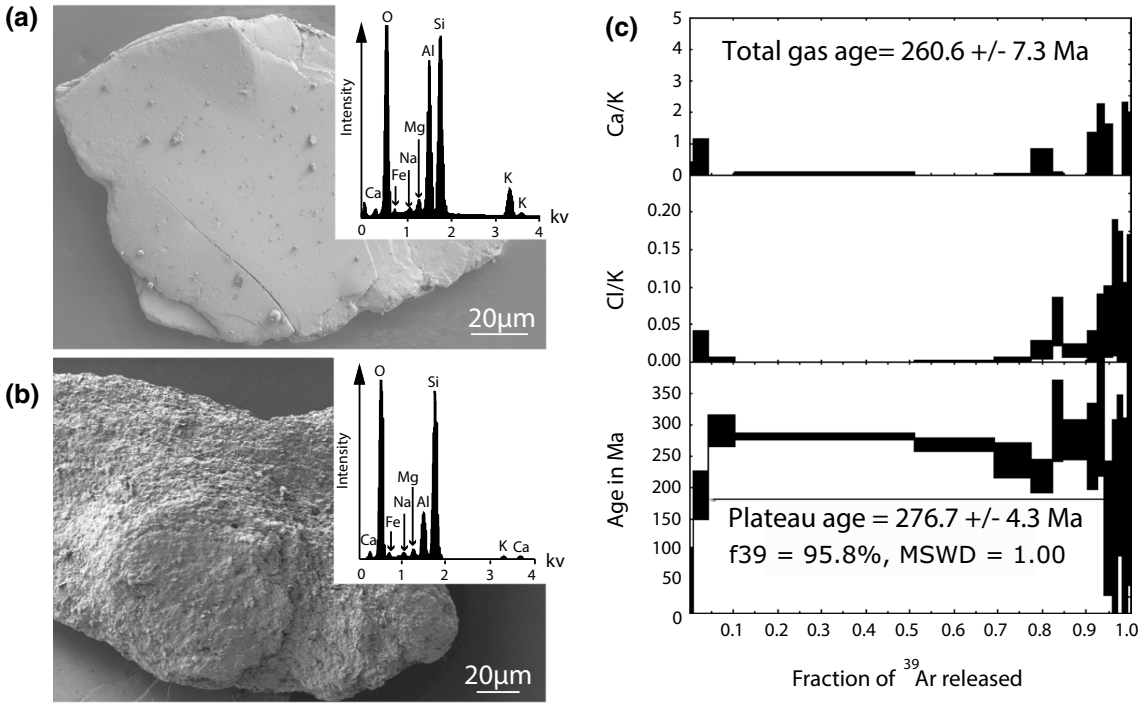

Fig. 5 **a** SEM image of a muscovite grain separated from the ash dyke. *Inset* shows the energy-dispersive spectrum containing abundant non-exchangeable K (average 8 % K_2O). **b** SEM image of a clay aggregate composed of Na-montmorillonite particles. The *inset* shows minor amounts of K occur in the interlayer, together with Na, Ca and Mg. **c** Laser-probe $^{40}Ar/^{39}Ar$ step-heating spectra of the separated mica fraction of an ash dyke sample (arg 2)

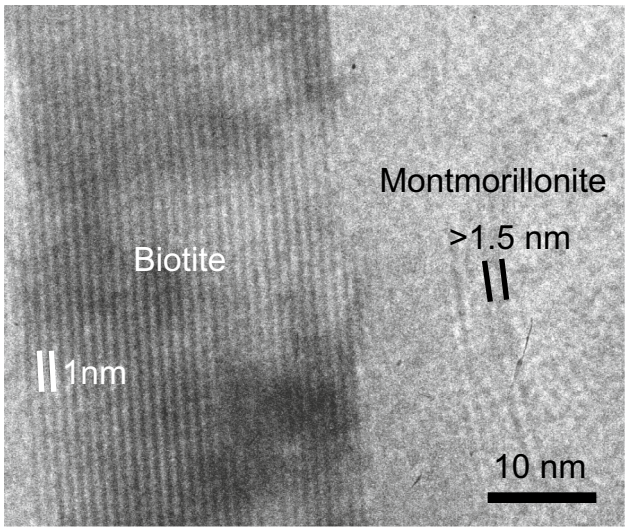

Fig. 6 Transmission electron lattice fringe image of the ash sample arg 2 showing a contact area between a mica crystal (here biotite) as the principle source of fixed K (1 nm) and thin montmorillonite particles (>1.5 nm) that contain minor amounts of exchangeable K. The expanded state of the montmorillonite was maintained by using LR white resin

to be of detrital origin (Fig. 5a). High-resolution lattice fringe images observed by transmission electron microscopy of the ash sample (arg 2) confirmed the occurrence of relatively unaltered mica crystals imbedded in a fine altered matrix composed of very thin, montmorillonite particles (Fig. 6). No mixed-layered structures were observed in the smectite packets in the sample studied, confirming the absence of interlayered illite at the lattice scale of observation.

The weight % of the <2-µm size fraction was also determined for the different rock types, whereby the finest lithologies are the bentonite (77–84 wt% is <2 µm) and mudstone (51–71 wt% is <2 µm) and the coarsest the ash dyke (27–36 wt% is <2 µm). Despite the fine-grained nature of the bentonite, thin Na-montmorillonite particles ranging up to 15 µm in diameter are observed by SEM, indicating a broad clay mineral particle size range for this lithology.

Quantification of exchangeable and fixed K content

The amount of exchangeable and fixed K content in the samples determined by cation exchange and XRF (Table 1) shows the lowest concentration of exchangeable K is present in the bentonite and almost all of the mudstones samples (K_2O 0.04–0.07 %; Table 2). The higher concentrations of exchangeable K in the ash samples, and the mudstone sample arg 9 (K_2O 0.10–0.20 %), may either reflect smectites with higher amounts of interlayer K, or alternatively undetected K stored in zeolites that is exchangeable. The

amount of fixed K follows a similar trend, which is lowest in the bentonite (K_2O 0.20–0.45 %) but has similar concentrations in all mudstones (K_2O 1.29–1.41 %) and ash samples (K_2O 1.34–1.42 %).

Quantification of mineral abundance using XRD methods did not produce satisfactory results due to the low intensities of the mica reflections and the problems of quantifying accurately smectite phases. Therefore, the amount of mica present was quantified chemically by determining the amount of K_2O in the detrital grains of the parent ash (8 % average, $n = 114$) and then dividing it by the amount of fixed K_2O present in the whole-rock samples (Table 1). This calculation assumes that all fixed K_2O is present in the detrital mica fraction and not in any other mineral phase. Repeat analyses indicate errors of 4–5 % are involved in this approach, assuming the average K-composition of the detrital mica phases in all lithologies is the same. The results indicate mica has an abundance of between 2.18 and 5.56 % in the bentonite, between 16.13 and 17.56 % in the mudstone and between 16.69 and 17.81 % in the ash (Table 2). The highest amount of mica occurring in the ash reflects the least altered state of this lithology, as indicated by the lower quantity of smectite formed. These calculations therefore indicate the amount of mica is similar in both the mudstone and ash samples, but is up to 6–7 times lower in concentration within the bentonite.

$^{40}Ar/^{39}Ar$ age of the detrital mica

The age of the mica phase (muscovite with minor biotite) that was hand-picked from an ash sample (arg 2) following wet sieving was evaluated from the $^{40}Ar/^{39}Ar$ spectrum (Fig. 5c: supplementary data A) whereby a plateau age of 276.7 ± 4.3 Ma (MSWD = 1, P value of 0.447) could be recognized and a total gas age (TGA) of 260.2 ± 7.3 Ma. Both ages indicate a source from Permian crystalline rocks. Due to the coarser grain size of the mica separates (160–250 μm), recoil effects are expected to be minimal and have no significant effect on the age analyses made. The TGA determined is considered to be the most compatible measurement consistent with the K–Ar results (Clauer et al. 2012; Clauer 2013) and was used in subsequent analyses. The given error of the TGA age is the propagation of errors determined by adding up all the error estimates of the individual gas fractions (supplementary data A). The mica in the ash is therefore confirmed as a clastic detrital mineral phase introduced during deposition.

K–Ar whole-rock ages of the volcaniclastic rocks

Overall the K–Ar whole-rock ages of the sampled volcaniclastic rocks range between 63.2 ± 3.0 and 115.0 ± 4.3 Ma. The youngest values are those of the bentonite samples (63.2 ± 3.0–76.7 ± 4.4 Ma), whereas the ash and mudstone samples have notably older ages with similar ranges, with the ash between 94.3 ± 4.0 and 113.8 ± 4.4 Ma and mudstone between 86.6 ± 3.5 and 115.0 ± 4.3 Ma. As all samples measured contain a mixture of fixed K in the mica phases, and exchangeable K in the montmorillonite, the measured results represent mixed ages values strongly influenced by the amount of detrital mica present. As the age of the end-member detrital mica has been determined in this study, the following section discusses the age of rock alteration using a procedure of analysis developed below.

Interpretation and discussion

Age analysis of Lago Pellegrini volcaniclastics

An age analysis of the untreated whole-rock powders of the Lago Pellegrini volcaniclastic samples was made by plotting the age function [exp(λt)-1] versus % detrital mica (%) and fitted using a York regression procedure (Mahon 1996; Fig. 7). The bentonite, ash and mudstones lithologies separately did not produce significantly different results, and therefore, this data set was combined. The high degree of correlation in this data set is reflected by a R^2 value of 0.97 for a best linear fit (supplementary data B). The intercept age from York regression analysis of 63.8 ± 1.7 Ma produces an end member for

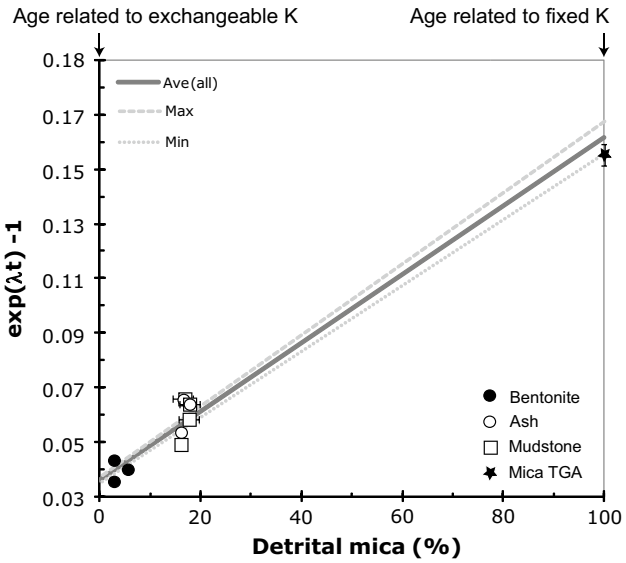

Fig. 7 Age analysis of the bentonite, ash and mudstone sample set. The exp (λt)—1 ages of 10 whole-rock powders (K–Ar results), and one mica separate ($^{40}Ar/^{39}Ar$: total gas age-TGA) is plotted against percent detrital mica content (%). The 0 % detrital mica intercept corresponds to the age of exchangeable K at 0.036 (63.8 ± 1.7 Ma). York regression errors are indicated and R^2 value of a best linear fit = 0.97

0 % detrital mica and hence no fixed K. That this end member has an age indicates that some if not all of the radiogenic Ar associated with this source of K was not lost since the isotopic closures of the system. Complete loss of this Ar would result in an intercept age of zero. The implication of this result is addressed in more detail by considering the characteristics of the rocks studied and their alteration history.

The bentonite, ash and mudstones contain an exchangeable K content of 0.04–0.2 %, which corresponds to published concentrations measured by cation exchange of similar montmorillonite-rich (>94 %) bentonites and associated rocks from the Lago Pellegrini (Iborra et al. 2006; Musso et al. 2010). As a K-bearing, Na-montmorillonite is also the dominant clay mineral phase in all of the samples we studied (Fig. 5b), there is little doubt that this mineral constitutes the main source of exchangeable K in these rocks. The small amounts of authigenic heulandite/clinoptilolite present in the ash samples could be another conceivable source of exchangeable K, although we failed to detect conclusively that this zeolite phase is K-bearing. Due to the absence of other minerals that may contain exchangeable K sources, it is considered unlikely that this isotopic signature originates from any volcanic mineral phases (ejecta) inherited from the parent ash material.

Purity of the smectite clay mineral phases

Another aspect of concern is whether or not interlayer illite layers are present in these smectite-dominated lithologies, which may influence the age analyses presented. Although XRD study and layer charge distribution measurements using the alkyl ammonium method did not detect any illite layers, we cannot totally exclude the presence of minor illite layers that lie below the detection limits of these methods (~<5 %). If some unidentifiable illite layers are present of authigenic origin, the fixed nature of the K will not contribute to the exchangeable K end-member age determined (Fig. 7) but instead influence the fixed K mica end-member age by making it relatively younger. However, due to the significantly older ages of the extrapolated detrital (Permian) mica age and the general absence of mixed-layered illite–smectite structures observed by X-ray diffraction study, layer charge determinations and transmission electron fringe imaging of selective samples, we consider the presence of such illite layers to be unlikely.

The absence of illite–smectite minerals in volcanoclastic rock sequences is not an unusual feature but is common to many industrial bentonites and parent ashes derived from Late Cretaceous to Tertiary volcanic deposits characterized by low K activities and low-temperature (<60 °C) burial histories (Christidis 2001; Christidis and Huff 2009). In fact, a similar mixture of authigenic Na-montmorillonite and detrital mica/and or illite of detrital origin is known for the well-studied Wyoming bentonite (Chipera and Bish 2001) of Cretaceous age. The absence of illite–smectite mixed layers in mudstone is, however, less common and probably reflects its volcaniclastic origin derived from similar material as that found in pyroclastic ash. The mudstone may also contain some reworked smectite from partly altered, underlying bentonite layers. The lack of authigenically formed illite layers is also perhaps not surprising considering the low total K_2O content of these samples (<1.62 %). In a study of the same mudstone sequence of the Allen Formation, Musso et al. (2010) did report a 1.0-nm basal spacing by XRD, which they interpreted to be a distinct "illite phase." As these authors did not study the nature of this phase in detail, we suggest that this reflection may be the same detrital micaceous material that we report from our sample set and in this case would not reflect a newly formed clay mineral phase.

Dating the age of smectite formation

Accepting that the intercept age (Fig. 7) represents exchangeable K located in smectite (montmorillonite) interlayers, and assuming the K-bearing detrital fraction has the same age in all samples studied, the meaning of this result can be considered in terms of smectite age dating. The bentonite samples characterized by the youngest K–Ar age values and lowest amount of detrital mica define a cluster of points close to the intercept age of the smectite at 63.8 ± 1.7 Ma. This end member overlaps with the less precise 63.2 ± 3.0 Ma age value of sample arg 11 (Table 1), which contains the lowest amount of mica contamination (~2.18 %) in the sample set studied. In contrast to the bentonite, the older K–Ar age values and higher detrital mica content of the parent ash and mudstone lithologies depart more significantly from the authigenic smectite end-member age, but fall along the same mixing line of authigenic and detrital components indicating they contain the same age of smectite, which if considering the analytical errors involved [~5 % (1σ), is significantly younger than the middle Campanian age of sedimentation (~80.3–76.2 Ma)].

It is a notable feature that the bentonite, ash and mudstone lithologies contain younger smectite with equivalent age despite significant differences in bulk rock mineralogy, grain size and extent of alteration and leaching. Whereas the bentonites contain high quantities of montmorillonite (>85 %) and clay-sized fraction (>77 wt%), this is in contrast to the parent ash dyke where montmorillonite is significantly less abundant, as is the clay-sized fraction (<36 wt%). The occurrence of zeolites in the preserved ash dyke also indicates restricted fluid–rock interaction compared to the extensive leaching of the bentonite layer (Christidis and Huff 2009). This appears to have had no resolvable influence on the age of smectite growth in this

rock sequence, even if some of the exchangeable K was to be located in the zeolite.

As the bentonite was formed by leaching of a glass-bearing pyroclastic ash during extensive fluid–rock interaction in an open system (Vallés and Giusiano 2001), loss of K and radiogenic ^{40}Ar gas likely occurred prior to eventual closure of the system. Extensive leaching of K is evident when comparing the composition of parent ash dyke and bentonite lithologies, with a 65–83 %, reduction in K, which represents a minimum estimate as the ash lithology is itself partly leached (Table 1). As the mechanism of smectite growth was dominated by dissolution and precipitation reactions, the cation content of the interlayer likely reflects the composition of the infiltrating fluids, which, in the case of Na-montmorillonites, are typically seawater-based formational fluids (Christidis and Huff 2009). In this context, the exchangeable K content of the smectite interlayers was governed by the composition of the permeating fluid and local dissolution of K-bearing glass phases and minerals (such as the muscovite, biotite and K-feldspars): conditions of which are considered ideal for removing any inherited radiogenic ^{40}Ar gas prior to the system closure.

The preferential loss or gain of excess radiogenic ^{40}Ar in these lithologies following smectite growth is considered unlikely in this very low-permeable rock sequence. Loss of ^{40}Ar after formation of the bentonite rock could conceivably occur during subsequent fluid–rock interaction, during sample preparation or during initial heating at 100 °C under high vacuum that was used to reduce atmospheric ^{36}Ar adsorbed on mineral surfaces prior to measurement of ^{40}Ar. ^{40}Ar loss by subsequent fluid–rock interaction associated with weathering can be ruled out as the samples were taken from freshly mined outcrops in cut sections well below the soil surface (>20 m), where wetting–drying cycles have minimum effect. Loss of radiogenic ^{40}Ar during sample preparation and experimental is similarly considered unlikely. None of the whole-sample powders used for isotopic analyses was subjected to contact with water that may have caused exchange reactions and loss of K or ^{40}Ar. If loss of ^{40}Ar occurred during reduction of ^{36}Ar during the initial heating in high vacuum, then this effect should show sample-specific variations, which is not the case. Differences in grain size between the three lithologies also offer no clear explanation whereby the bentonite and mudstone lithologies are both very fine-grained lithologies compared to the ash dyke. Therefore, grain size-dependent losses could not explain the age equivalence of the coarser ash material and the finer tuffaceous mudstones. In contrast to loss, any excess radiogenic ^{40}Ar would be expected to result in unusually old samples, probably older than the age of sedimentation, which is not observed. Such secondary changes would also be expected to induce differences related to the degree of leaching that occurred.

Isotopic closure of the bentonite and mudstone lithologies and implications for the underground disposal of nuclear waste

The formation and isotopic closure of bentonite rock can be expected to be complete above ~60 % smectite content when very low hydraulic conductivities are attained ($<10^{-11}$ m^2/s) and the rate of solute transport is reduced to the rate of molecular diffusion (Lehikoinen et al. 1996). It has been demonstrated in similar Na-montmorillonite-rich bentonites that, when nanopores reach dimensions <10 nm in size, the seal also becomes impermeable to the flow of fluids (Horseman et al. 1999), which is ideal for the retention of radiogenic argon whether in dissolved or gaseous form. Another aspect favorable for retention is the absence of subsequent alteration of the lithologies marked by the lack of illite growth or any other reactions that may have led to elemental gain or loss. The lack of elemental mobility would also imply that recrystallization of the smectite is also unlikely under these conditions. Therefore, since the time of isotopic closure at 63.8 ± 1.7 Ma, the mostly impermeable bentonite layer is expected to have retained its radiogenic ^{40}Ar, with no exchange or fractionation of K except by ^{40}K decay. These conditions are considered suitable for dating of the completion of authigenic montmorillonite growth in the Lake Pellegrini bentonite. Therefore, adopting the age of middle Campanian sedimentation (~80.3–76.2 Ma), the termination of montmorillonite growth and isotopic closure of the bentonite is proposed to have occurred ~13–17 my after deposition of the parent ash. This relatively long time period of bentonite formation is, however, dependent on the accuracy of the stratigraphic age, which in this case has been inferred from paleontological assemblages. Dating more precisely the age of sedimentation by U–Pb dating of zircons extracted from these volcanic ash deposits could further improve the time constraints presented.

Although the precise amount of smectite present in the mudstone lithologies was not determined, the high abundance of smectite in these samples implies also that high enough quantities formed to seal the unit. This was confirmed by swelling tests of selected whole-rock samples whereby the smectitic mudstones placed in water swelled equally to those of the bentonites. This is in accordance with the results of Musso et al. (2010), who determined ~75–85 % montmorillonite for this lithology and thus considered these rocks to have equivalent properties to the interbedded bentonites. As the measured hydraulic conductivity of saturated clay powders was reported to be as low as 1.3×10^{-12} and 7.0×10^{-13} m/s, for mudstone and bentonite samples, respectively, the conductivities of the intact whole rocks and associated microporosities can be expected to be significantly lower. The ash lithology,

however, with its low smectite content, is notably more porous, but at this location it is considered likely that after intrusion into the overlying volcaniclastic sediments, it was effectively sealed by smectite growth in the mudstones and not by reactions within the ash itself that was inhibited by limited fluid–rock interaction.

It is proposed that smectite-dominated, very low-permeability materials (bentonite and mudstone layers) studied here serve as preferred sinks for the accumulation of radioactive argon, and show similar Ar retention properties as observed for smectite, illite and glauconite minerals during experimental heating (Odin and Bonhomme 1982; Hassanipak and Wampler 1996). This feature has important implications for dating smectites in geological environments and provides a method for understanding the currently unknown time period required to form high-purity Na-montmorillonitic bentonite and smectite-based mudstone deposits. Although the initial alteration of reactive glass-rich ash deposits is generally viewed as a rapid process when subjected to saline to supersaline waters (Hay and Gludman 1987), in the case of the Lago Pellegrini, volcaniclastic rocks studied show a particularly long period of smectite growth (up to 13–17 my) probably related to continuing fluid–rock interaction and protracted leaching within the buried volcaniclastic sedimentary sequence. This provides a novel constraint on the time required to convert a pyroclastic ash into a Na-bentonite deposit.

The age of isotopic closure of clay alteration zones may be dateable when containing low-permeability smectite, including hydrothermally altered oceanic crust (Alt et al. 1992) or hemipelagic sediments (Turner et al. 1993), fault gouge (Janssen et al. 2013) or diagenetic mudrocks that have not undergone illitization (April 1981). Our approach also provides a rigorous test for the effectiveness of geological closure when considering the suitability of smectitic-based host rocks for nuclear waste storage, which can constitute effective barriers for preventing migration of fluids (Horseman et al. 1999; Harrington and Horseman 1999). In this case study, the naturally compacted bentonite rock has remained effectively sealed since the early Tertiary. Based on our results, therefore, we conclude that the age of smectite growth and closure of a system can, in some cases, be constrained with the procedure documented in this study.

Conclusions

1. Radiogenic ^{40}Ar caused by the decay of exchangeable ^{40}K in smectite was retained in the low-permeability volcaniclastic rocks of the Lago Pellegrini, Northern Patagonian. This can be used to date smectite precipitation and closure of the system by a combined K–Ar and $^{40}Ar/^{39}Ar$ age analytical procedure.
2. Age analysis of the Lago Pellegrini bentonite and associated rocks deposited during the Late Cretaceous middle Campanian stage (stratigraphic age 83.6 ± 0.2 and 72.1 ± 0.2 Ma) indicates a time period of 13–17 my was required to complete smectite precipitation and formation of the bentonite deposit, as well as alteration of parent ash and mudstone lithologies of volcaniclastic origin.
3. Smectite age analysis is proposed as a useful method for accessing the closure history of low-permeability volcaniclastic and clastic rocks and may aid the assessment of the suitability of clay-rich lithologies for the underground storage of nuclear waste.
4. Successful dating of smectite by K–Ar analysis requires that exchangeable K is present at detectable concentrations and that all fixed K is present as mica that can be dated independently.

Acknowledgments Raymond Wendling of the former Centre de la Geochimie de la Surface in Strasbourg (ULP-CNRS) is thanked for K–Ar isotopic analyses and Chris Hall (Uni-Michigan) for $^{40}Ar/^{39}Ar$ analysis of the mica sample. Manfred Zander's help with the electron microscopy analyses is also acknowledged. The study was supported by the DFG, Wa 803/4-1 (LNW) and the National Science Foundation, EAR-1118704 (BvdP). Georg Grathoff and Peter Vrolijk are thanked for helpful comments on an early version of the manuscript. We also acknowledge the feedback of Masafumi Sudo (Uni-Potsdam) and an anonymous reviewer for their constructive input that led to improvement of this paper.

References

Aguirre-Urreta B, Tunik M, Naipauer M, Pazos P, Ottone E, Fanning M, Ramos VA (2011) Malargüe Group (Maastrichtian–Danian) deposits in the Neuquén Andes, Argentina: implications for the onset of the first Atlantic transgression related to Western Gondwana break-up. Gondwana Res 19:482–494. doi:10.1016/j.gr.2010.06.008

Alt JC, France-Lanord C, Floyd PA, Paterno C, Galy A (1992) Low-temperature hydrothermal alteration of Jurassic ocean crust, Site 801. In: Larson R, Lancelot Y et al (eds) Proceedings of the ocean drilling program, scientific results, College Station, TX (Ocean Drilling Program), vol 129, pp 415–427. doi:10.2973/odp.proc.sr.129.132.1992

April RH (1981) Trioctahedral smectite and interstratified chlorite/smectite in Jurassic strata of the Connecticut Valley. Clays Clay Miner 29:31–39. doi:10.1346/CCMN.1981.0290105

Aronson JL, Douthitt CB (1986) K/Ar systematic of an acid-treated illite/smectite: implications for evaluating age and crystal structure. Clays Clay Miner 34:473–482. doi:10.1346/ccmn.1986.0340414

Bechtel A, Elliott WC, Wampler JM, Oszczepalski S (1999) Clay mineralogy, crystallinity, and K–Ar ages of illites within the Polish Zechstein Basin; implications for the age of Kupferschiefer mineralization. Econ Geol 94:261–272. doi:10.2113/gsecongeo.94.2.261

Bergaya F, Lagaly G, Vayer M (2006) Cation and anion exchange. In: Bergaya F, Theng BKG, Lagaly G (eds) Developments in clay science. Elsevier, Amsterdam, pp 979–1001. doi:10.1016/S1572-4352(05)01036-6

Bonhomme MG, Thuizat R, Pinault Y, Clauer N, Wendling R, Winkler R (1975) Methode de datation potassium—argon. Appareillage et Technique (The potassium—argon dating method). Notes technique de l'Institut de Géologie, Université Louis Pasteur, Strasbourg, 3, 53 pp

Chipera SJ, Bish DL (2001) Baseline studies of the clay minerals society source clays: powder X-ray diffraction analyses. Clays Clay Miner 49:398–409. doi:10.1346/CCMN.2001.0490507

Christidis GE (2001) Formation and growth of smectites in bentonites: a case study from Kimolos Island, Aegean, Greece. Clays Clay Miner 49:204–215. doi:10.1346/ccmn.2001.0490303

Christidis GE, Huff WD (2009) Geological aspects and genesis of bentonites. Elements 5:93–98. doi:10.2113/gselements.5.2.93

Clauer N (2013) The K–Ar and $^{40}Ar/^{39}Ar$ methods revisited for dating fine-grained K-bearing clay minerals. Chem Geol 354:163–185. doi:10.1016/j.chemgeo.2013.05.030

Clauer N, Giblin P, Lucas J (1984) Sr and Ar isotope studies of detrital smectite from the Atlantic ocean (D.S.D.P., Legs 43, 48 and 50). Isot Geosci 2:141–151. doi:10.1016/0009-2541(84)90185-2

Clauer N, Zwingmann H, Liewig N, Wendling R (2012) Comparative 40Ar/39 Ar and K–Ar dating of illite-type clay minerals: a tentative explanation for age identities and differences. Earth Sci Rev 115:76–96. doi:10.1016/j.earscirev.2012.07.003

Dalrymple GB, Lanphere MA (1969) Potassium—argon dating. Freeman, San Francisco

Gasparini Z, Casadio S, Fernàndez M, Salgodo L (2001) Marine reptiles from the Late Cretaceous of northern Patagonia. J South Am Earth Sci 14:51–60. doi:10.1016/S0895-9811(01)00012-8

Gradstein FM, Ogg JG, Smith AG (eds) (2004) A geologic time scale 2004. Cambridge University Press, Cambridge. doi:10.1017/s001675680521141x

Grathoff G, Moore D (1996) Illite polytype quantification using WILDFIRE—calculated patterns. Clays Clay Miner 44:835–842. doi:10.1346/ccmn.1996.0440615

Haines SH, van der Pluijm BA (2008) Clay quantification and Ar–Ar dating of synthetic and natural gouge: application to the Miocene Sierra Mazatán detachment fault, Sonora, Mexico. J Struct Geol 30:525–538. doi:10.1016/j.jsg.2007.11.012

Harrington JF, Horseman ST (1999) Gas transport properties of clays and mudrocks. In: Aplin AC, Fleet AJ, Macquaker JHS (eds) Muds and mudstones: physical and fluid flow properties. Geol Soc Lond Spec Publ 158:107–124. doi:10.1144/gsl.sp.1999.158.01.09

Hassanipak AA, Wampler JM (1996) Radiogenic argon released by stepwise heating of glauconite and illite: the influence of composition and particle size. Clays Clay Miner 44:717–726. doi:10.1346/ccmn.1996.0440601

Hay RL, Gludman SG (1987) Diagenetic alteration of silicic ash in Searles Lake, California. Clays Clay Miner 35:449–457. doi:10.1346/ccmn.1987.0350605

Hazen RM, Sverjensky DA, Azzolini D, Bish D, Elmore SC, Hinnov L, Milliken RE (2013) Clay mineral evolution. Am Mineral 98:2007–2029. doi:10.2138/am.2013.4425

Hofmann H (2003) Einfluss konzentrierter Salzlösungen auf die physiko-chemischen Eigenschaften quellfähiger Tonminerale: Konsequenzen für den Einsatz von Bentonit als Versatzmaterial in einem Endlager für schwach- und mittelradioaktive Abfälle in Salzformationen. Dissertation of the University of Heidelberg, 140 pp

Hofmann H, Bauer A, Warr LN (2002) XCharge—ein Programm zur Berechnung der Schichtladung und Schichtladungsverteilung niedrig geladener Phyllosilikate mit Hilfe der Alkylammonium-Methode: Grundlagen und Benutzerhandbuch. Band 6744 von Forschungszentrum Karlsruhe Technik und Umwelt, Wissenschaftliche Berichte, 25 pp

Horseman ST, Harrington JF, Sellin P (1999) Gas migration in clay barriers. Eng Geol 54:139–149. doi:10.1016/S0013-7952(99)00069-1

Howell JA, Schwarz E, Spalletti L, Veiga GD (2005) The Neuquén Basin: an overview. In: Veiga GD, Spalletti LA, Howell JA, Schwarz E (eds) The Neuquén Basin, Argentina: a case study in sequence stratigraphy and basin dynamics. Geol Soc Lond Spec Publ 252:1–14. doi:10.1144/gsl.sp.2005.252.01.01

Hunziker JC, Frey M, Clauer N, Dallmeyer RD, Friedrichsen H, Flehming W, Hochstrasser K, Roggwiller P, Schwander H (1986) The evolution of illite to muscovite: mineralogical and isotopic data from the Glarus Alps, Switzerland. Contrib Mineral Petrol 92:157–180. doi:10.1007/BF00375291

Iborra CV, Cultrone G, Cerezo P, Aguzzi C, Baschini MT, Vallés J, López-Galindo A (2006) Characterisation of northern Patagonian bentonites for pharmaceutical uses. Appl Clay Sci 31:272–281. doi:10.1016/j.clay.2005.11.002

Impiccini A (1995) Mineralogía de la fracción no arcillosa de las bentonitas del Cretácico superior de la región Norpatagonia. PhD thesis, Univ. Nac. La Plata

Janssen C, Wirth R, Lin A, Dresen G (2013) TEM microstructural analysis in a fault gouge sample of the Nojima Fault Zone, Japan. Tectonophysics 583:101–104. doi:10.1016/j.tecto.2012.10.020

Kim J, Peacor DR, Tessier D, Elsass F (1995) A technique for maintaining texture and permanent expansion of smectite interlayers for TEM observations. Clays Clay Miner 43:51–57. doi:10.1346/ccmn.1995.0430106

Lagaly G (1994) Layer charge determination by alkylammonium ions. In: Mermut AR (ed) Layer charge characteristics of 2:1 silicate clay minerals. CMS workshop lectures. Clay Min Soc 6:1–46. doi:10.1346/cms-wls-6.1

Lagaly G, Weiss A (1971) Anordnung und Orientierung kationischer Tenside auf Silicatoberflächen. Teil IV: Anordnung von n-Alkylammoniumionen bei niedrig geladenen Schichtsilicaten. Kolloid Z Z Polym 243:48–55. doi:10.1007/bf01500614

LeBas MJ, LeMaitre RW, Streckeisen A, Zanettin B (1986) A chemical classification of volcanic rocks based on the total alkali–silica diagram. J Petrol 27:745–750. doi:10.1093/petrology/27.3.745

Lehikoinen J, Carlsson J, Muurinen A, Olin M, Salonen P (1996) Evaluation of factors affecting diffusion in compacted bentonite. Mater Res Soc Symp Proc 412:675–682. doi:10.1557/proc-412-675

LoBello P, Feraud G, Hall CM, York D, Lavina P, Bernat M (1987) $^{40}Ar/^{39}Ar$ step-heating and laser fusion dating of a quaternary volcanic from Neschers, Massif Central, France: the defeat of xenocrystic contamination. Chem Geol 66:61–71. doi:10.1016/0168-9622(87)90029-7

Lombardi B, Baschini M, Torres-Sánchez RM (2003) Bentonite deposits of northern Patagonia. Appl Clay Sci 22:309–312. doi:10.1016/j.clay.2005.11.002

Mahon K (1996) The new "York" regression; application of an improved statistical method to geochemistry. Int Geol Rev 38:293–303. doi:10.1080/00206819709465336

McDougall I, Harrison TM (1999) Geochronology and thermochronology by the $^{40}Ar/^{39}Ar$ method, 2nd edn. Oxford University Press, Oxford. doi:10.1093/petrology/41.12.1823

Mermut AR, Lagaly G (2001) Baseline studies of the clay minerals society source clays: layer-charge determination and characteristics of those minerals containing 2:1 layers. Clays Clay Miner 49:393–397. doi:10.1346/ccmn.2001.0490506

Moore DM, Reynolds RC Jr (1997) X-ray diffraction and the identification and analysis of clay minerals, 2nd edn. Oxford University Press, Oxford. doi:10.1017/s0016756898501501

Musso TB, Roehl KE, Pettinari G, Vallés JM (2010) Assessment of smectite-rich claystones from North Patagonia for their

use as liner materials in landfills. Appl Clay Sci 48:438–445. doi:10.1016/j.clay.2010.02.001

Nauman TE, Crawford Elliott W, Wampler JM (2012) K–Ar age constraints on the origin of micaceous minerals in Savannah River Site Soils, South Carolina, USA. Clays Clay Miner Minerals 60:496–506. doi:10.1346/ccmn.2012.0600506

Odin GS (1982) Interlaboratory standards for dating purposes. In: Odin GS (ed) Numerical dating in stratigraphy. Wiley, New York, pp 123–149. doi:10.1016/1359-0189(90)90126-i

Odin GS, Bonhomme MG (1982) Argon behaviour in clays and glauconies during preheating experiments. In: Odin GS (ed) Numerical dating in stratigraphy. Wiley, New York, pp 333–343

Pevear DR (1992) Illite age analysis, a new tool for basin thermal history analysis. In: Kharaka YK, Maest AS (eds) Proceedings of the 7th international symposium on water-rock interaction. Balkema, Rotterdam, Netherlands, pp 1251–1254

Smith JV, Yoder HS Jr (1956) Experimental and theoretical studies of the mica polymorphs. Mineral Mag 31:209–331. doi:10.1180/minmag.1956.031.234.03

Solum JG, van der Pluijm BA, Peacor DR, Warr LN (2003) Influence of phyllosilicate mineral assemblages, fabrics, and fluids on the behavior of the Punchbowl fault, southern California. J Geophys Res Solid Earth 108(B5):2233. doi:10.1029/2002JB001858

Środoń J, Morgan DJ, Eslinger EV, Eberl DD, Karlinger MR (1986) Chemistry of illite/smectite and end-member illite. Clays Clay Miner 34:368–378. doi:10.1346/ccmn.1986.0340403

Szczerba M, Środoń J (2009) Extraction of diagenetic and detrital ages and of the ^{40}Kdetrital/^{40}Kdiagenetic ratio from K–Ar dates of clay fraction. Clays Clay Miner 57:93–103. doi:10.1346/ccmn.2009.0570109

Turner RJW, Ames DE, Franklin JM, Goodfellow WD, Leitch CHB, Höy T (1993) Character of active hydrothermal mounds and nearby altered hemipelagic sediments in the hydrothermal areas of Middle Valley, Northern Juan de Fuca Ridge: data on shallow cores. Can Miner 31:973–999. doi:10.4095/132633

Vallés JM, Giusiano A (2001) Bentonitic and kaolin deposits in extra-Andean Patagonia and soils in the Andean region. Post-conference field excursion July 29–August 1st, 2001. In: The 12th international clay conference, Universida Nacional de sur Bahia Blanca- Argentina, 59 pp

Vallés JM, Burlando L, Chiachiarini P, Giaveno M, Impiccini A (1989) Geological and genetical features of the Upper Cretaceous bentonite deposit from North Patagonia. PICG, 24, Cretácico América Latina, Buenos Aires, pp 79–98

van der Pluijm B, Hall C, Vrolijk P, Pevear D, Covey M (2001) The dating of shallow faults in the Earth's crust. Nature 412:172–175. doi:10.1038/35084053